

# NJC

Accepted Manuscript



This is an *Accepted Manuscript*, which has been through the Royal Society of Chemistry peer review process and has been accepted for publication.

*Accepted Manuscripts* are published online shortly after acceptance, before technical editing, formatting and proof reading. Using this free service, authors can make their results available to the community, in citable form, before we publish the edited article. We will replace this *Accepted Manuscript* with the edited and formatted *Advance Article* as soon as it is available.

You can find more information about *Accepted Manuscripts* in the [Information for Authors](#).

Please note that technical editing may introduce minor changes to the text and/or graphics, which may alter content. The journal's standard [Terms & Conditions](#) and the [Ethical guidelines](#) still apply. In no event shall the Royal Society of Chemistry be held responsible for any errors or omissions in this *Accepted Manuscript* or any consequences arising from the use of any information it contains.



## ARTICLE

## Luminescence, energy transfer and tunable color of Ce<sup>3+</sup>, Dy<sup>3+</sup>/Tb<sup>3+</sup> doped BaZn<sub>2</sub>(PO<sub>4</sub>)<sub>2</sub> phosphors

Luxiang Wang,<sup>a</sup> Mengjiao Xu,<sup>a</sup> Hongyang Zhao<sup>a</sup> and Dianzeng Jia<sup>\*a</sup>

Received 00th January 20xx,  
Accepted 00th January 20xx

DOI: 10.1039/x0xx00000x

www.rsc.org/

Ce<sup>3+</sup>, Dy<sup>3+</sup> and Tb<sup>3+</sup> doped BaZn<sub>2</sub>(PO<sub>4</sub>)<sub>2</sub> phosphors were prepared by a high temperature solid state reaction route. The crystal structure, photoluminescence properties, decay lifetime, luminous efficiency and thermal stability of the phosphors were investigated. The mechanism of Ce<sup>3+</sup>-Dy<sup>3+</sup>/Tb<sup>3+</sup> energy transfer was determined to be a dipole-dipole interaction based on the photoluminescence spectra and decay curves of the phosphors. The critical distance between the Ce<sup>3+</sup> and Dy<sup>3+</sup>/Tb<sup>3+</sup> ion were calculated by both the concentration quenching method and the spectral overlap method. Tunable emission from blue to bluish white and green can be realized by energy transfer and changing the doping concentrations of Dy<sup>3+</sup> and Tb<sup>3+</sup> under the UV light. The BaZn<sub>2</sub>(PO<sub>4</sub>)<sub>2</sub>: Ce<sup>3+</sup>, Dy<sup>3+</sup>/Tb<sup>3+</sup> phosphors are proved to be promising candidates in lighting field due to their excellent thermal stability and luminescence properties.

### 1. Introduction

Rare earth activated inorganic compounds have been widely recognized as important luminescence materials in fluorescent lamp, light emitting diodes, field emission displays and cathode ray tubes<sup>1-4</sup>. Compared with the conventional incandescent and fluorescent lamp, light emitting diodes have attracted significant attention thanks to their high luminous efficiency, low energy consumption, low pollution and long lifetime. A lot of research work has been carried out on the phosphors, which are the key components in luminescent devices. The synthesis, crystal structure, luminescence properties and related luminescence mechanisms of different types of phosphor materials have been reported<sup>5,6</sup>. The phosphors are the key components in the process of luminescent device fabrication. Hence, the development of novel phosphors has attracted a lot of attention in recent years.

It is well known that energy transfer plays an important role in tuning color emission in phosphors<sup>7,8</sup>. As an important activator for phosphors, Dy<sup>3+</sup> ion has a 4f<sup>9</sup> electron configuration, and usually exhibits two main emissions in the visible region: one in the blue region (470-500 nm) and one in the yellow region (570-600 nm), which originate from <sup>4</sup>F<sub>9/2</sub>-<sup>6</sup>H<sub>15/2</sub> and <sup>4</sup>F<sub>9/2</sub>-<sup>6</sup>H<sub>13/2</sub> transitions of Dy<sup>3+</sup> ions, respectively<sup>9-13</sup>. Meanwhile, the trivalent Tb<sup>3+</sup> ions are usually used as a green emitting activator based on their relatively simple

structure of energy levels that consists of <sup>7</sup>F<sub>J</sub>, <sup>5</sup>D<sub>4</sub>, and <sup>5</sup>D<sub>3</sub> states<sup>14-16</sup>. However, Dy<sup>3+</sup> and Tb<sup>3+</sup> ions involving 4f-4f spin forbidden transitions are usually not favorable for luminescence because the 4f electronic shell is regularly shielded by the 5d electronic shell. Accordingly, the emission lines of spectra are narrow, and the emission intensity is rather weak, which is not beneficial for full spectra emitting and applications in phosphors. In order to enhance the absorption of Dy<sup>3+</sup>/Tb<sup>3+</sup> in the UV region, one of the most effective methods is to introduce sensitizer (such as Ce<sup>3+</sup>, Eu<sup>2+</sup>) to transfer its absorption energy to the activator. The Ce<sup>3+</sup> ion could exhibit a broadband emission located at broader ranges from UV to the visible region due to its 4f-5d parity allowed electric dipole transition. Based on this, Ce<sup>3+</sup> ions can serve as good sensitizer in the co-doped materials, and transfer a part of their energy to activator ions. This kind of energy transfer has been reported in a number of Ce<sup>3+</sup>-Dy<sup>3+</sup> and Ce<sup>3+</sup>-Tb<sup>3+</sup> co-doped phosphors, for example, 12CaO · 7Al<sub>2</sub>O<sub>3</sub>: Ce<sup>3+</sup>, Dy<sup>3+</sup>, SrZnP<sub>2</sub>O<sub>7</sub>: Ce<sup>3+</sup>, Dy<sup>3+</sup>, Li<sub>2</sub>SrGeO<sub>4</sub>: Ce<sup>3+</sup>, Dy<sup>3+</sup>/Tb<sup>3+</sup>, Y<sub>4</sub>Si<sub>2</sub>N<sub>2</sub>O<sub>7</sub>: Ce<sup>3+</sup>, Tb<sup>3+</sup>, Dy<sup>3+</sup>, CaGdGaAl<sub>2</sub>O<sub>7</sub>: Ce<sup>3+</sup>, Tb<sup>3+</sup>, Ca<sub>6</sub>Ba(PO<sub>4</sub>)<sub>4</sub>O: Ce<sup>3+</sup>/Tb<sup>3+</sup><sup>17-24</sup>.

MZn<sub>2</sub>(PO<sub>4</sub>)<sub>2</sub> (M=Mg, Ca, Sr, Ba), an important family of host with low costs, low synthetic temperature, high luminous efficiency and excellent thermal stability, have gained increasing interest in the investigations of luminescent materials, such as MgZn<sub>2</sub>(PO<sub>4</sub>)<sub>2</sub>: Eu<sup>2+</sup>/Eu<sup>3+</sup>, SrZn<sub>2</sub>(PO<sub>4</sub>)<sub>2</sub>: Eu<sup>2+</sup>, Mn<sup>2+</sup>, SrZn<sub>2</sub>(PO<sub>4</sub>)<sub>2</sub>: Tb<sup>3+</sup>, Li<sup>+</sup>, BaZn<sub>2</sub>(PO<sub>4</sub>)<sub>2</sub>: Sm<sup>3+</sup><sup>25-28</sup>. In order to enrich the color of the emitted light and improve the luminescent performance, it is necessary to choose other dopant ions for BaZn<sub>2</sub>(PO<sub>4</sub>)<sub>2</sub> phosphor materials. To the best of our knowledge, the luminescence properties and energy transfer between Ce<sup>3+</sup> and Dy<sup>3+</sup>/Tb<sup>3+</sup> in BaZn<sub>2</sub>(PO<sub>4</sub>)<sub>2</sub> host lattice have not been reported so far.

In the present work, we synthesized Ce<sup>3+</sup>, Dy<sup>3+</sup>, Tb<sup>3+</sup> doped BaZn<sub>2</sub>(PO<sub>4</sub>)<sub>2</sub> phosphors via high temperature solid state reaction

<sup>a</sup> Key Laboratory of Energy Materials Chemistry (Xinjiang University), Ministry of Education, Key Laboratory of Advanced Functional Materials, Autonomous Region, Institute of Applied Chemistry, Xinjiang University, Urumqi 830046, Xinjiang, PR China

† Corresponding author: \*E-mail: jdz@xju.edu.cn/jdz0991@gmail.com Tel.: +86-991-8583083; Fax: +86-991-8588883

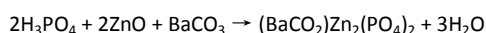
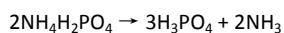
Electronic Supplementary Information (ESI) available: [details of any supplementary information available should be included here]. See DOI: 10.1039/x0xx00000x

route. The photoluminescence properties and energy transfer mechanism of  $\text{Ce}^{3+}$  to  $\text{Dy}^{3+}/\text{Tb}^{3+}$  in the  $\text{BaZn}_2(\text{PO}_4)_2$  host under UV light have been studied in detail. On the basis of energy transfer, the emission color can be tuned from blue to bluish white and green by adjusting the relative ratio of  $\text{Ce}^{3+}$  and  $\text{Dy}^{3+}/\text{Tb}^{3+}$ .

## 2. Experimental

### 2.1 Synthesis

The phosphors  $\text{BaZn}_2(\text{PO}_4)_2 \cdot x\text{Ce}^{3+} \cdot y\text{Dy}^{3+} / z\text{Tb}^{3+}$  ( $0 \leq x \leq 0.12$ ,  $0.0025 \leq y \leq 0.03$ ,  $0.005 \leq z \leq 0.06$ ) were synthesized by a solid state reaction method. Analytical grade  $\text{BaCO}_3$ ,  $\text{ZnO}$ ,  $\text{NH}_4\text{H}_2\text{PO}_4$ ,  $\text{CeO}_2$ ,  $\text{Dy}_2\text{O}_3$  and  $\text{Tb}_4\text{O}_7$  were used as starting materials without further purification. Stoichiometric mixtures of the starting materials were homogeneously ground, which was then calcined at  $950^\circ\text{C}$  for 3 h in reductive atmosphere. The effect of calcining temperature and holding time on the luminescent properties of the samples are shown in Fig. S1. The final products were obtained after cooling down to room temperature naturally.  $\text{BaZn}_2(\text{PO}_4)_2$  compound was formed according to the following chemical reactions:



### 2.2 Characterization

Powder X-ray diffraction (XRD) measurements were performed on a Bruker D8 Advance Diffraction diffractometer in the  $2\theta$  range from  $10^\circ$  to  $80^\circ$  with  $\text{Cu K}\alpha$  radiation ( $\lambda = 0.15405\text{ nm}$ ) at 40 kV, 40 mA. The excitation and emission spectra were recorded on a Hitachi F-4500 spectrometer equipped with a 150 W xenon lamp as the excitation source. The luminescence decay curves were obtained from a Lecroy Wave Runner 6100 Digital Oscilloscope (1 G Hz) using a tunable laser (pulse width=4 ns, gate= 50 ns) as the excitation source (Continuum Sunlite OPO). Fluorescent thermal stability of the phosphors was analyzed using a HORIBA Jobin Yvon Fluorolog-3 instrument.

## 3. Results and discussion

A series of  $\text{Ce}^{3+}$ ,  $\text{Dy}^{3+}/\text{Tb}^{3+}$  co-doped  $\text{BaZn}_2(\text{PO}_4)_2$  phosphors were synthesized by a solid state reaction method. In order to understand the detailed energy transfer process between  $\text{Ce}^{3+}$  and  $\text{Dy}^{3+}/\text{Tb}^{3+}$ , we investigated the crystal structure, photoluminescence properties, decay lifetime, luminous efficiency and thermal stability of the phosphors.

### 3.1 Phase analysis

The phase composition and purity of the as-prepared powder samples were analyzed by XRD. Fig. 1 shows the XRD patterns of  $\text{Ce}^{3+}/\text{Dy}^{3+}/\text{Tb}^{3+}$  single- or co-doped  $\text{BaZn}_2(\text{PO}_4)_2$  (designated as BZPO) samples. All the reflections of these samples are in agreement with the BZPO host and can be indexed to the JCPDS card (No. 16-0554). No additional peaks from other phases were detected, indicating that a single phase has formed and the doping of  $\text{Ce}^{3+}/\text{Dy}^{3+}/\text{Tb}^{3+}$  ion does not significantly influence the crystal structure of BZPO.

BZPO has a monoclinic crystal structure with a space group of  $\text{P}2_1/c$ , and the lattice parameters are  $a=8.598\text{ \AA}$ ,  $b=9.761\text{ \AA}$ ,  $c=9.159\text{ \AA}$ , and  $V=768.45\text{ \AA}^3$ . The unit cell has five crystallographically independent cation sites, i.e., one seven-coordinated  $\text{Ba}^{2+}$  sites, two four-coordinated  $\text{Zn}^{2+}$  site, and two four-coordinated  $\text{P}^{5+}$  sites (see Fig. 2). Zinc and phosphorus tetrahedral build up a three dimensional network isotopic to the hurlbutite-type  $\text{CaBe}_2(\text{PO}_4)_2$ <sup>29,30</sup>. The barium atoms form isolated  $\text{BaO}_7$  polyhedra located between large octagonal holes.

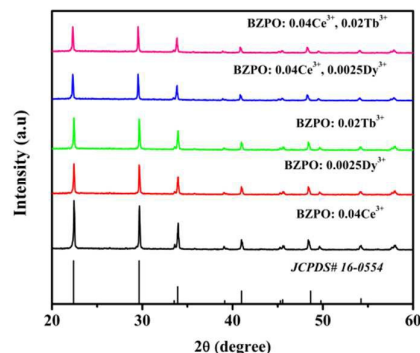


**Fig. 1** XRD patterns of samples BZPO: 0.04 $\text{Ce}^{3+}$ , BZPO: 0.0025 $\text{Dy}^{3+}$ , BZPO: 0.02 $\text{Tb}^{3+}$ , BZPO: 0.04 $\text{Ce}^{3+}$ , 0.0025 $\text{Dy}^{3+}$  and BZPO: 0.04 $\text{Ce}^{3+}$ , 0.02 $\text{Tb}^{3+}$ .

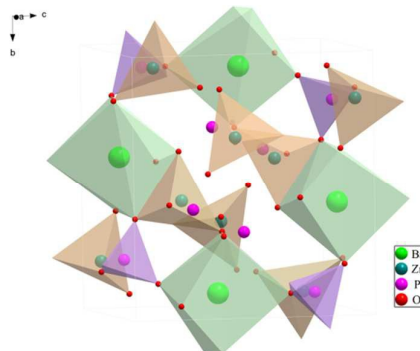


**Fig. 2** Schematic illustration of the crystal structure of  $\text{BaZn}_2(\text{PO}_4)_2$ .

Based on the effective ionic radii of cations with different coordination numbers, we propose that  $\text{Ce}^{3+}/\text{Dy}^{3+}/\text{Tb}^{3+}$  are expected to occupy the  $\text{Ba}^{2+}$  sites preferably, since the ionic radii of  $\text{Ce}^{3+}/\text{Dy}^{3+}/\text{Tb}^{3+}$  is close to that of  $\text{Ba}^{2+}$  (see Tab. S1), while the  $\text{Zn}^{2+}$  and  $\text{P}^{5+}$  sites with ionic radii of 0.68 and 0.17  $\text{Å}$ , respectively, are too small for  $\text{Ce}^{3+}$ ,  $\text{Dy}^{3+}/\text{Tb}^{3+}$  cations to occupy. In this case, substitution of  $\text{Ce}^{3+}/\text{Dy}^{3+}/\text{Tb}^{3+}$  cations could result in positive charges in the lattices [ $\text{Ce}_{\text{Ba}}$ ], [ $\text{Dy}_{\text{Ba}}$ ] or [ $\text{Tb}_{\text{Ba}}$ ]. The mismatch of charge on the cation sites could be balanced by negative charges, for example, vacancy of cation: [ $\text{V}_{\text{Ba}}$ ] or interstitial oxygen [ $\text{O}_i$ ]<sup>28</sup>.

### 3.2 Photoluminescence properties

Fig. 3 shows the emission and excitation spectra of BZPO: 0.04 $\text{Ce}^{3+}$ , BZPO: 0.0025 $\text{Dy}^{3+}$ , BZPO: 0.02 $\text{Tb}^{3+}$ , BZPO: 0.04 $\text{Ce}^{3+}$ , 0.0025 $\text{Dy}^{3+}$  and BZPO: 0.04 $\text{Ce}^{3+}$ , 0.02 $\text{Tb}^{3+}$ . The excitation band of BZPO: 0.04 $\text{Ce}^{3+}$  (Fig. 3a) monitored at 326 nm in the region from 200 to 320 nm, which can be attributed to the transitions from the ground state to the different crystal field splitting levels of the 5d state of the  $\text{Ce}^{3+}$  ions. Under UV excitation of 280 nm, the emission spectrum of the BZPO: 0.04 $\text{Ce}^{3+}$  sample displays an asymmetric

emission band ranging from 290 to 500 nm with a maximum at about 326 nm. Because of the spin-orbit splitting of the ground state  $^2F_{5/2}$  and  $^2F_{7/2}$  with an energy difference of about  $2000\text{ cm}^{-1}$ , the emission spectrum for the  $\text{Ce}^{3+}$  doped phosphor usually has doublet character. The dependence curve of emission intensity on the contents of  $\text{Ce}^{3+}$  in BZPO phosphor was shown in Fig. S2. It can be seen that the emission intensities increase with increasing  $\text{Ce}^{3+}$  concentrations, and then decrease. At about  $x=0.04$ , the maximum emission intensity occurs.

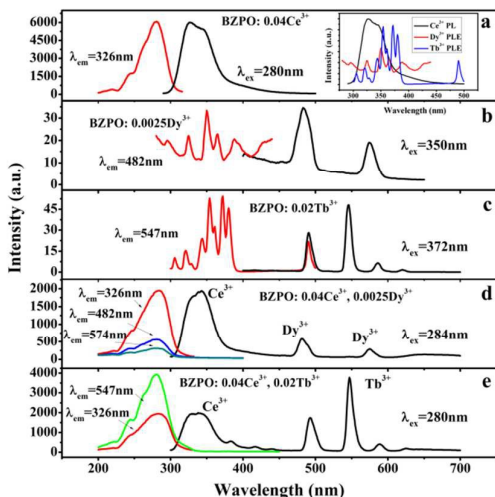


**Fig. 3** Excitation and emission spectra of phosphors: (a) BZPO:  $0.04\text{Ce}^{3+}$ , (b) BZPO:  $0.0025\text{Dy}^{3+}$ , (c) BZPO:  $0.02\text{Tb}^{3+}$ , (d) BZPO:  $0.04\text{Ce}^{3+}$ ,  $0.0025\text{Dy}^{3+}$ , (e) BZPO:  $0.04\text{Ce}^{3+}$ ,  $0.02\text{Tb}^{3+}$ . The inset Fig. 3a shows the spectral overlap between the emission spectrum of BZPO:  $0.04\text{Ce}^{3+}$  and the excitation spectrum of BZPO:  $0.0025\text{Dy}^{3+}/0.02\text{Tb}^{3+}$ .

The excitation and emission spectra of the BZPO:  $0.0025\text{Dy}^{3+}$  sample are presented in Fig. 3b. The excitation spectrum monitored at 482 nm shows several sharp peaks at 324 nm, 350 nm, 364 nm, 388 nm, 428 nm, which can be attributed  $^6\text{H}_{15/2}-^7\text{F}_{5/2}$ ,  $^6\text{H}_{15/2}-^6\text{P}_{5/2}$ ,  $^6\text{H}_{15/2}-^6\text{P}_{7/2}$ ,  $^6\text{H}_{15/2}-^4\text{F}_{7/2}$ ,  $^6\text{H}_{15/2}-^4\text{G}_{11/2}$ , respectively. Under excitation at 350 nm, the emission spectrum exhibits two sharp peaks located at 482 nm and 574 nm due to the  $^4\text{F}_{9/2}-^6\text{H}_{15/2}$  and  $^4\text{F}_{9/2}-^6\text{H}_{13/2}$  transitions, respectively. It well known that the  $\text{Dy}^{3+}$  emission around 482 nm ( $^4\text{F}_{9/2}-^6\text{H}_{15/2}$ ) derives from its magnetic dipole transition and the emission around 574 nm ( $^4\text{F}_{9/2}-^6\text{H}_{13/2}$ ) originates from its electric dipole transition. It is observed that the  $^4\text{F}_{9/2}-^6\text{H}_{15/2}$  transition is dominant in the host, which implies that the  $\text{Dy}^{3+}$  ions locate at low symmetry sites with no inversion centers. The excitation and emission spectra of  $\text{Tb}^{3+}$  activated BZPO powders are shown in Fig. 3c. The excitation spectrum of the BZPO:  $0.02\text{Tb}^{3+}$  monitored at 547 nm displays several bands between 300 and 400 nm, which can be attributed to f-f transitions within the  $4f^8$  configuration of  $\text{Tb}^{3+}$ . The emission peaks at 490 nm, 547 nm, 582 nm, 621 nm were observed under excitation at 372 nm corresponding to the  $^5\text{D}_4-^7\text{F}_j$  ( $j=6, 5, 4, 3$ ) transitions of  $\text{Tb}^{3+}$ .

It can be seen from Fig. 3b and Fig. 3c that the f-f transitions of  $\text{Dy}^{3+}$  and  $\text{Tb}^{3+}$  ions are very weak and cannot absorb UV light effectively. However, the 5d-4f transition of  $\text{Ce}^{3+}$  is electric dipole allowed and can strongly absorb UV light. When  $\text{Ce}^{3+}$  and  $\text{Dy}^{3+}$  (or  $\text{Tb}^{3+}$ ) ions are co-doped into the BZPO host, the energy transfer from  $\text{Ce}^{3+}$  to  $\text{Dy}^{3+}$

(or  $\text{Tb}^{3+}$ ) ions are expected to occur upon UV excitation. The inset in Fig. 3a shows that there is an overlap between the emission band of  $\text{Ce}^{3+}$  and the f-f absorptions of  $\text{Dy}^{3+}/\text{Tb}^{3+}$ . According to the formula given by Dexter<sup>31,32</sup>:

$$P_{SA} = 2\pi / h \left| \langle S, A^* | H_{SA} | S^*, A \rangle \right|^2 \int_{SA} g_S(E) g_A(E) dE \quad (1)$$

where  $P_{SA}$  and  $H_{SA}$  are the energy transfer rate and the interaction Hamiltonian, respectively; the matrix element indicates the interaction between the initial state  $|S^*, A\rangle$  and the final state  $\langle S, A^*|$ . The integral represents the spectral overlap between the emission spectrum of the sensitizers and the excitation spectrum of activators. From the observed spectral overlap between the emission band of  $\text{Ce}^{3+}$  and the excitation of  $\text{Dy}^{3+}/\text{Tb}^{3+}$  in Fig. 3a and the eqn (1), it can be concluded that resonance type energy transfer may occur from  $\text{Ce}^{3+}$  to  $\text{Dy}^{3+}/\text{Tb}^{3+}$  in the BZPO host. This can be further confirmed by the excitation and emission spectra of BZPO:  $\text{Ce}^{3+}$ ,  $\text{Dy}^{3+}$  and BZPO:  $\text{Ce}^{3+}$ ,  $\text{Tb}^{3+}$  in Fig. 3d and 3e. Under the excitation at 284 nm, the emission spectrum of BZPO:  $\text{Ce}^{3+}$ ,  $\text{Dy}^{3+}$  not only exhibits  $^2\text{D}_{3/2}-^2\text{F}_{7/2}$  emission band of the  $\text{Ce}^{3+}$  ions but also shows the  $^4\text{F}_{9/2}-^6\text{H}_{15/2}/^6\text{H}_{13/2}$  emission of the  $\text{Dy}^{3+}$  ions. The excitation spectra of BZPO:  $0.04\text{Ce}^{3+}$ ,  $0.0025\text{Dy}^{3+}$  are obtained by monitoring the emission at 326 nm, 482 nm, 574 nm, respectively. The three excitation spectra present similar shapes with different peak intensities, and the strongest peak is located at 284 nm. Similarly, the emission spectrum of BZPO:  $0.04\text{Ce}^{3+}$ ,  $0.02\text{Tb}^{3+}$  (see Fig. 3e) excitation at 280nm yields both the weak emission of  $\text{Ce}^{3+}$  (300 nm-360 nm,  $^2\text{D}_{3/2}-^2\text{F}_{5/2}/^2\text{F}_{7/2}$ ) and the strong emission of  $\text{Tb}^{3+}$  (480 nm-680 nm,  $^5\text{D}_4-^7\text{F}_j$ ,  $j=6, 5, 4, 3$ ). Additionally, comparing the emission intensity of BZPO:  $\text{Dy}^{3+}/\text{Tb}^{3+}$  and the corresponding BZPO:  $\text{Ce}^{3+}$ ,  $\text{Dy}^{3+}/\text{Tb}^{3+}$  with the same  $\text{Dy}^{3+}/\text{Tb}^{3+}$  doping concentration, the emission intensities of  $\text{Dy}^{3+}/\text{Tb}^{3+}$  of the latter are much higher than those of the former. In other words, the emission intensities of BZPO:  $\text{Dy}^{3+}/\text{Tb}^{3+}$  can be enhanced by co-doping  $\text{Ce}^{3+}$  ions into the BZPO host via energy transfer.

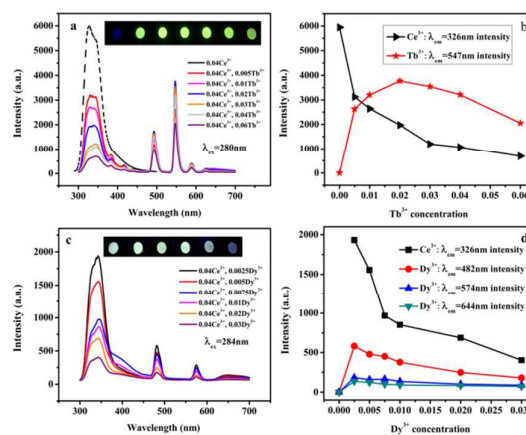


**Fig. 4** Emission spectra of BZPO:  $0.04\text{Ce}^{3+}$ ,  $z\text{Tb}^{3+}$  (a), BZPO:  $0.04\text{Ce}^{3+}$ ,  $\gamma\text{Dy}^{3+}$  (c), and the variation of the emission intensities of  $\text{Ce}^{3+}$  and  $\text{Tb}^{3+}/\text{Dy}^{3+}$  versus the  $\text{Tb}^{3+}$  (b) /  $\text{Dy}^{3+}$  (d) concentration. The inset Fig. 5a and 5c shows the digital luminescence photographs under a 254 UV lamp excitation.

A series of  $\text{Ce}^{3+}$ ,  $\text{Tb}^{3+}/\text{Dy}^{3+}$  co-doped phosphors was synthesized by fixing the  $\text{Ce}^{3+}$  concentration at 0.04 and modifying

the Dy<sup>3+</sup> concentration (y) and Tb<sup>3+</sup> concentration (z). Fig. 4a shows the variation of emission spectra of BZPO: 0.04Ce<sup>3+</sup>, zTb<sup>3+</sup> (z=0~0.06) phosphors with different Tb<sup>3+</sup> concentrations. The emission intensities of Ce<sup>3+</sup> decrease with increasing Tb<sup>3+</sup> concentration, while the emission intensities of Tb<sup>3+</sup> increase firstly, and then reach a maximum at the Tb<sup>3+</sup> concentration of 0.02 before decreasing gradually with further increase of Tb<sup>3+</sup> concentration due to concentration quenching. Fig. 4b shows the variation of the emission intensities of Ce<sup>3+</sup> and Tb<sup>3+</sup> versus the Tb<sup>3+</sup> concentration. The observed variations of the emission intensity of the Ce<sup>3+</sup> and Tb<sup>3+</sup> ions indicate that the energy transfer process occurred from Ce<sup>3+</sup> to Tb<sup>3+</sup>. The variation of the emission intensities of the Ce<sup>3+</sup> and Dy<sup>3+</sup> shows a similar tendency as compared to the Ce<sup>3+</sup>-Tb<sup>3+</sup> system (Fig. 4c). The emission intensities of Ce<sup>3+</sup> declines with an increased Dy<sup>3+</sup> concentration, when the value of y reaches 0.0025, the maximum emission intensity of Dy<sup>3+</sup> occurs (Fig. 4d). According to the above results, the optimal composition of Ce<sup>3+</sup> and Tb<sup>3+</sup>/Dy<sup>3+</sup> co-activated phosphors are BZPO: 0.04Ce<sup>3+</sup>, 0.02Tb<sup>3+</sup> and BZPO: 0.04Ce<sup>3+</sup>, 0.0025Dy<sup>3+</sup>, which show the strongest emission. The emission colors of the BZPO: 0.04Ce<sup>3+</sup>, zTb<sup>3+</sup>/yDy<sup>3+</sup> phosphors can be adjusted from blue to green and from blue to white, respectively (see inset in Fig. 4a and 4c).

### 3.3 Energy transfer mechanism

In order to understand the detailed energy transfer process between Ce<sup>3+</sup> and Dy<sup>3+</sup>/Tb<sup>3+</sup>, we investigated the energy transfer mechanism of the Ce<sup>3+</sup>-Dy<sup>3+</sup>/Tb<sup>3+</sup> in the BZPO host. Fig. 5a and 5b present the decay lifetime of Ce<sup>3+</sup> in the BZPO: 0.04Ce<sup>3+</sup>, yDy<sup>3+</sup> and BZPO: 0.04Ce<sup>3+</sup>, zTb<sup>3+</sup> samples monitored at 342 nm with different Dy<sup>3+</sup> and Tb<sup>3+</sup> concentrations. The decay curve of Ce<sup>3+</sup> ions can be well fitted to a single-exponential function. As described by Blasse and Grabmaier<sup>31, 32</sup>, the decay behavior of Ce<sup>3+</sup> ions can be expressed by:

$$I = I_0 \exp\left(1 - \frac{t}{\tau}\right) \quad (2)$$

where  $I_0$  and  $I$  are the luminescence intensity of Ce<sup>3+</sup> at time 0 and  $t$ , respectively, and  $\tau$  is the decay lifetime. The lifetimes of Ce<sup>3+</sup> in BZPO: 0.04Ce<sup>3+</sup>, yDy<sup>3+</sup> phosphors were calculated to be 49.35, 44.56, 44.23, 40.18, 34.51, 30.97 and 22.56 ns for y=0, 0.0025, 0.005, 0.0075, 0.01, 0.02 and 0.03, respectively. The lifetimes of Ce<sup>3+</sup> in BZPO: 0.04Ce<sup>3+</sup>, zTb<sup>3+</sup> phosphors were calculated to be 49.35, 47.71, 47.14, 39.78, 39.34, 37.57 and 34.46 ns for z=0, 0.005, 0.01, 0.02, 0.03, 0.04 and 0.06, respectively. It is worth noting that the decay lifetimes of Ce<sup>3+</sup> decrease with the increase of Dy<sup>3+</sup> and Tb<sup>3+</sup> concentration, which is convictive evidence for the energy transfer from Ce<sup>3+</sup> to Dy<sup>3+</sup> and Tb<sup>3+</sup> ions in the BZPO host. Generally, the energy transfer efficiency ( $\eta_T$ ) from the sensitizer to the activator can be estimated by Equation (3):

$$\eta_T = 1 - \frac{\tau}{\tau_0} \quad (3)$$

where the  $\tau$  and  $\tau_0$  are the luminescence lifetime of the sensitizer Ce<sup>3+</sup> ions with and without the presence of the activator Dy<sup>3+</sup>/Tb<sup>3+</sup>, respectively. The energy transfer efficiencies are plotted as a function of the Dy<sup>3+</sup>/Tb<sup>3+</sup> concentration and are shown in Fig. 6a and 6b. Under excitation at 280 nm, the energy transfer efficiencies for

Ce<sup>3+</sup>-Dy<sup>3+</sup> and Ce<sup>3+</sup>-Tb<sup>3+</sup> can reach 50 % and 30 % with y=0.03 and z=0.06, respectively.

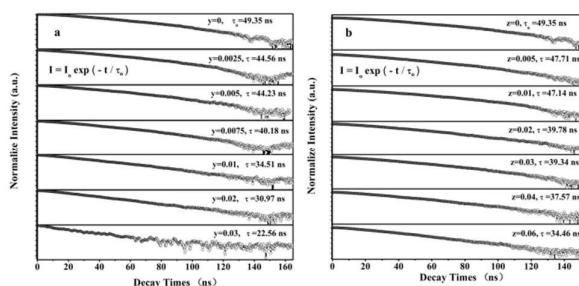


**Fig. 5** The lifetime decay curves of Ce<sup>3+</sup> in the BZPO: 0.04Ce<sup>3+</sup>, yDy<sup>3+</sup> (a) and BZPO: 0.04Ce<sup>3+</sup>, zTb<sup>3+</sup> (b) samples.

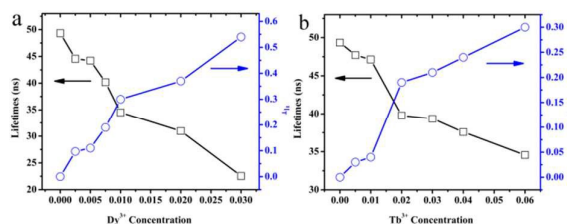


**Fig. 6** Dependence of the luminescence lifetime of Ce<sup>3+</sup> and energy transfer efficiency ( $\eta_T$ ) on the doped concentration of Dy<sup>3+</sup> ions (a) and Tb<sup>3+</sup> ions (b).

Usually, the concentration quenching is frequently caused by energy transfer from one activator to another, until an energy sink in the lattice is reached. The critical distance  $R_c$  for energy transfer between the Ce<sup>3+</sup> and Dy<sup>3+</sup>/Tb<sup>3+</sup> ions were calculated using the concentration quenching method by the following equation given by Blasse<sup>32</sup>:

$$R_c \approx 2 \left[ \frac{3V}{4\pi XZ} \right]^{1/3} \quad (4)$$

where  $V$  is the volume of the unit cell,  $Z$  is the number of formula units per unit cell, and  $X$  is the critical concentration of dopant ions. For the BZPO host,  $V = 768.45 \text{ \AA}^3$ ,  $Z=4$ , and  $X$  is 0.0425 and 0.06 for Ce<sup>3+</sup>-Dy<sup>3+</sup> and Ce<sup>3+</sup>-Tb<sup>3+</sup>, respectively. According to equation (4), the critical distance  $R_c$  is estimated to be about 20.52 Å and 18.29 Å. In general, there are three mechanisms for non-radiate energy transfer including exchange interaction, radiation reabsorption and electric multipolar interactions. It is hardly possible that the energy transfer through long distances of more than 5 Å for the exchange interaction mechanism. The mechanism of radiation reabsorption is only efficacious when the fluorescence and absorption spectra are strongly overlapping, which is also not the case in this work. Consequently, we can conclude the energy transfer mechanism between Ce<sup>3+</sup> and Dy<sup>3+</sup>/Tb<sup>3+</sup> ions belongs to electric multipolar interactions.

On the basis of Dexter's energy transfer formula of multi-polar interaction and Reisfeld's approximation, the following relation can be given<sup>33-35</sup>:

$$\eta_0/\eta \propto C^{n/3} \quad (5)$$

Where  $\eta_0$  and  $\eta$  are the luminescence quantum efficiency of the sensitizer Ce<sup>3+</sup> in the absence and presence of the activator Dy<sup>3+</sup>/Tb<sup>3+</sup>;  $C$  is the sum of the content of Ce<sup>3+</sup> and Dy<sup>3+</sup>/Tb<sup>3+</sup>;  $n=6, 8$ ,

and 10 corresponding to dipole-dipole, dipole-quadrupole and quadrupole-quadrupole interactions, respectively. The value  $\eta_0/\eta$  is approximately calculated by the ratio of related luminescence intensities as:

$$I_{50}/I_5 \propto C^{n/3} \quad (6)$$

Where  $I_{50}$  is the intrinsic luminescence intensity of  $Ce^{3+}$ ,  $I_5$  the luminescence intensity of  $Ce^{3+}$  in the presence of the  $Dy^{3+}/Tb^{3+}$ . The  $I_{50}/I_5 - C^{n/3}$  plots are shown in Fig. 7, and the relation is observed when  $n=6, 8,$  and  $10$ . It can be find that all the biggest  $R^2$  values of the linear fittings occur when  $n=6$ , corresponding to their best linear behaviors. Therefore, the energy transfer from the  $Ce^{3+}$  to  $Dy^{3+}/Tb^{3+}$  ions occurs through the electric dipole-dipole interaction mechanism.

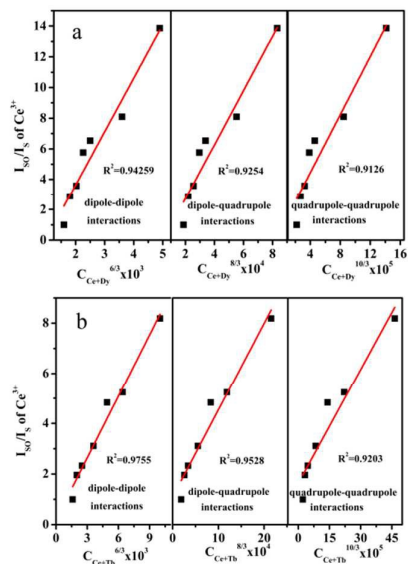


**Fig. 7**  $I_{50}/I_5$  versus  $C^{n/3}$  plots of the  $Ce^{3+}$ ,  $Dy^{3+}$  (a) and the  $Ce^{3+}$ ,  $Tb^{3+}$  (b) co-doped phosphors.

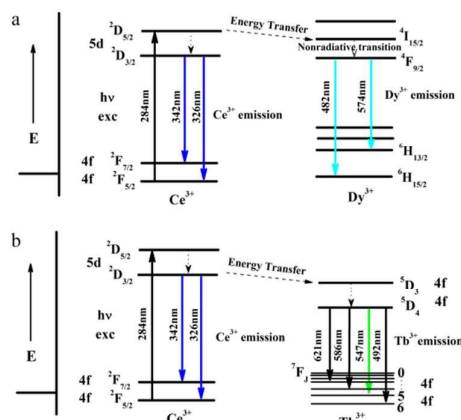
According to Dexter's energy transfer theory, the energy transfer process through multi-polar interaction depends on the extent of overlap between the emission spectrum of the sensitizer and the absorption spectrum of the activator, the relative orientation of interacting dipoles and the distance between the sensitizer and the activator. For dipole-dipole interaction, the energy transfer probability  $P_{SA}$  (in  $s^{-1}$ ) from a sensitizer to an acceptor is given by the following equation<sup>7-32, 35</sup>:

$$P_{SA} = 3.024 \times 10^{12} \frac{f_d}{R_c^6 \tau_s} \int \frac{f_s(E)F_A(E)}{E^4} dE \quad (7)$$

where  $f_d$  is the oscillator strength of the involved absorption transition of the acceptor ( $Dy^{3+}/Tb^{3+}$ ),  $\tau_s$  is the radiative decay time of the sensitizer (in seconds),  $R_c$  is the sensitizer-acceptor average distance (in Å),  $E$  is the energy involved in the transfer (in eV) and represents the spectral overlap between the normalized shapes of the  $Ce^{3+}$  emission  $f_s(E)$  and the  $Dy^{3+}/Tb^{3+}$  excitation  $F_A(E)$ . The critical distance ( $R_c$ ) of energy transfer from the sensitizer to the acceptor is defined as the distance for which the probability of transfer equals the probability of radiative emission of donor, the distance for which  $P_{SA} \tau_s = 1$ . Hence,  $R_c$  can be obtained from eq (8) as

$$R_c^6 = 3.024 \times 10^{12} f_d \int \frac{f_s(E)F_A(E)}{E^4} dE \quad (8)$$

The  $f_d$  electric dipole oscillator strength of the  $Dy^{3+}$  and  $Tb^{3+}$  ions are usually referred to be order of  $2.5 \times 10^{-6}$  and  $1.0 \times 10^{-6}$ , respectively<sup>36, 37</sup>. Using these values and calculated spectral overlap, the critical distance  $R_c$  for a dipole-dipole interaction mechanism are 21.69 Å and 19.07 Å. These results are in good agreement with those obtained using the concentration quenching method (20.52 Å and 18.29 Å), which confirms that the mechanism of energy transfer from  $Ce^{3+}$  to  $Dy^{3+}/Tb^{3+}$  ions is mainly due to a dipole-dipole interaction.



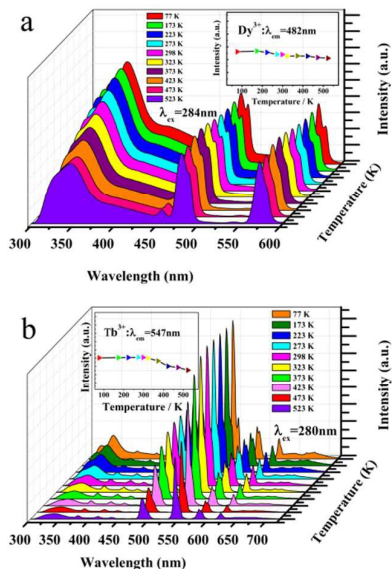
**Fig. 8** The illustration of the energy transfer modes for a:  $Ce^{3+}$ - $Dy^{3+}$ ; b:  $Ce^{3+}$ - $Tb^{3+}$ .

Fig. 8 illustrates the energy levels of  $Ce^{3+}$ ,  $Dy^{3+}$ ,  $Tb^{3+}$  and the energy transfer processes from  $Ce^{3+}$  to  $Dy^{3+}/Tb^{3+}$ . Under excitation with UV light (See Fig. 8a), electrons are excited from the ground state  $^2F_{5/2}$  to the excited state  $^2D_{5/2}$  of  $Ce^{3+}$  and non-radiatively relaxed to the lowest component of the 5d level. Subsequently, decay to the  $^2F_{5/2}$  and  $^2F_{7/2}$  levels occurs via a radiation process emitting photons. Other photons transfer the excitation energy to the excited levels of  $Dy^{3+}$  ( $^4I_{15/2}$ ), which is ascribed to similar energy level, followed by cross relaxation to the  $^4F_{9/2}$  level of  $Dy^{3+}$ , and further by a radiative transition to  $^6H_{15/2}$  (blue) and  $^6H_{13/2}$  (yellow) levels. The energy transfer between  $Ce^{3+}$  and  $Tb^{3+}$  is similar (See Fig. 8b): the  $^5D_3$  level of  $Tb^{3+}$  receives the transferred energy from excited  $Ce^{3+}$ , and then relaxes to the  $^5D_4$  level of  $Tb^{3+}$ . Finally, a set of characteristic optical transitions  $^5D_4 \rightarrow ^7F_J$ , located at about 492 nm, 547 nm, 586 nm and 621 nm (corresponding to  $J=6, 5, 4, 3$ ) occur.

### 3.4. Thermal stability and CIE coordinates

One of the key requirements for a good phosphor is to maintain the performance at the operating temperature of the device. Usually, the luminescence intensity of the phosphors at 423 K with respect to that at room temperature is used to assess the thermal stability. Fig. 9a and 9b show the temperature dependence of the emission of BZPO: 0.04 $Ce^{3+}$ , 0.0025 $Dy^{3+}$  and BZPO: 0.04 $Ce^{3+}$ , 0.02 $Tb^{3+}$  excited at 284 nm and 280 nm, respectively. The emission intensity decreased slightly with increasing temperature since the probability of thermally activated crossover from the excited state to the ground state, causing the thermal quenching. A decay of 8% and 20% for the BZPO: 0.04 $Ce^{3+}$ , 0.0025 $Dy^{3+}$  and BZPO: 0.04 $Ce^{3+}$ , 0.02 $Tb^{3+}$  at 423 K were observed, indicating that the phosphors

have a relatively good thermal stability against the thermal quenching effect. In addition, the emission wavelength shows no shifts with increasing temperature from 77 K to 523 K.



**Fig. 9** Emission spectra of BZPO: 0.04Ce<sup>3+</sup>, 0.0025Dy<sup>3+</sup> (a) and BZPO: 0.04Ce<sup>3+</sup>, 0.02Tb<sup>3+</sup> (b) phosphors at a temperatures range from 77K to 523K.

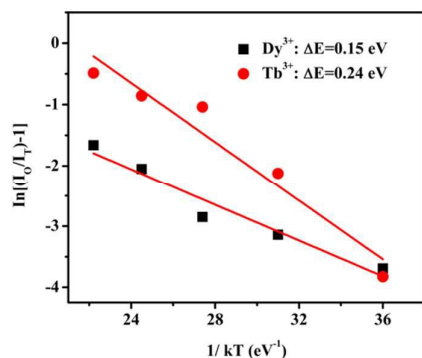


**Fig. 10** A  $\ln(I_0/I_T - 1) - 1/kT$  activation energy graph for thermal quenching of Dy<sup>3+</sup>/Tb<sup>3+</sup> in BZPO: Ce<sup>3+</sup>, Dy<sup>3+</sup>/Tb<sup>3+</sup> phosphor.

In order to verify the origin of temperature dependent emission intensity ( $I_T$ ), the activation energy ( $\Delta E$ ) was calculated using the Arrhenius equation<sup>38</sup>:

$$I_T = I_0 / \left[ 1 + c \exp\left(-\frac{\Delta E}{kT}\right) \right] \quad (9)$$

where  $I_0$  is the initial emission intensity of the phosphor at room temperature,  $I_T$  is the emission intensity at different temperatures,  $c$  is a constant,  $\Delta E$  is the activation energy of thermal quenching, and  $k$  is Boltzmann constant ( $k=8.62 \times 10^{-5}$  eV). According to the equation, the activation energy  $\Delta E$  can be calculated from a plotting of  $\ln(I_0/I_T - 1)$  against  $1/kT$ , where the straight slope equals  $-\Delta E$ . As shown in Fig. 10,  $\Delta E$  were calculated to be 0.15 eV and 0.24 eV for Dy<sup>3+</sup> and Tb<sup>3+</sup>, respectively. The relatively high activation energy results in a good thermal stability for this phosphor. Therefore, the phosphor showed an excellent thermal stability and

outstanding luminescence properties, indicating that the BZPO: Ce<sup>3+</sup>, Dy<sup>3+</sup>/Tb<sup>3+</sup> phosphor has high potentials in light emitting field.

The CIE chromaticity coordinates of the BZPO: xCe<sup>3+</sup>, yDy<sup>3+</sup>/zTb<sup>3+</sup> phosphors with different dopant contents were measured according to their luminescence spectra and presented in Fig. 11, and the x and y values of CIE chromaticity coordinates are shown in Tab. 1. The CIE chromaticity coordinates of the Ce<sup>3+</sup>, Dy<sup>3+</sup> and Tb<sup>3+</sup> single doped BZPO: 0.04Ce<sup>3+</sup>, BZPO: 0.0025Dy<sup>3+</sup> and BZPO: 0.02Tb<sup>3+</sup> phosphors are (0.1542, 0.0300), (0.2448, 0.2742) and (0.2874, 0.5153) corresponding to dark blue, bluish white and green emission, respectively. However, the emission color of Ce<sup>3+</sup> and Dy<sup>3+</sup> co-doped phosphors could be changed from blue and cyan to bluish white by adjusting the doping concentrations of Dy<sup>3+</sup>. The CIE chromaticity coordinate associated with white luminescence (0.2964, 0.2914) of BZPO: 0.04Ce<sup>3+</sup>, 0.0025Dy<sup>3+</sup> sample is very close to an ideal white chromaticity coordinates (0.33, 0.33). In addition, the CIE chromaticity coordinate of the optimized BZPO: 0.04Ce<sup>3+</sup>, 0.02Tb<sup>3+</sup> phosphor is calculated to be (0.2640, 0.5450), which is closer to the commercial phosphor MgAl<sub>11</sub>O<sub>19</sub>: 0.67Ce<sup>3+</sup>, 0.33Tb<sup>3+</sup> (0.3300, 0.5950), indicating that the BZPO: 0.04Ce<sup>3+</sup>, 0.02Tb<sup>3+</sup> phosphor has a suitable color coordinate as a green phosphor for lighting field.

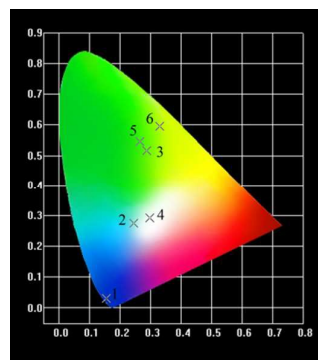


**Fig. 11** CIE chromaticity diagram for BZPO: xCe<sup>3+</sup>, yDy<sup>3+</sup>/zTb<sup>3+</sup> phosphors: (1) x=0.04, y=0; (2) x=0, y=0.0025; (3) x=0, z=0.02; (4) x=0.04, y=0.0025; (5) x=0.04, z=0.02, (6) MgAl<sub>11</sub>O<sub>19</sub>: 0.67Ce<sup>3+</sup>, 0.33Tb<sup>3+</sup>.

**Table 1.** The CIE chromaticity coordinates of BZPO: xCe<sup>3+</sup>, yDy<sup>3+</sup>/zTb<sup>3+</sup> (x=0, 0.04, y=0, 0.0025, z=0, 0.02) under UV excitation.

Point	Sample	CIE (x, y)
1	BZPO: 0.04Ce <sup>3+</sup> ( $\lambda_{ex}=280$ nm)	(0.1542, 0.0300)
2	BZPO: 0.0025Dy <sup>3+</sup> ( $\lambda_{ex}=350$ nm)	(0.2448, 0.2742)
3	BZPO: 0.02Tb <sup>3+</sup> ( $\lambda_{ex}=372$ nm)	(0.2874, 0.5153)
4	BZPO: 0.04Ce <sup>3+</sup> , 0.0025Dy <sup>3+</sup> ( $\lambda_{ex}=284$ nm)	(0.2964, 0.2914)
5	BZPO: 0.04Ce <sup>3+</sup> , 0.02Tb <sup>3+</sup> ( $\lambda_{ex}=280$ nm)	(0.2640, 0.5450)
6	MgAl <sub>11</sub> O <sub>19</sub> : 0.67Ce <sup>3+</sup> , 0.33Tb <sup>3+</sup>	(0.3300, 0.5950)

#### 4. Conclusions

In summary, a series of BaZn<sub>2</sub>(PO<sub>4</sub>)<sub>2</sub> phosphors doped by Ce<sup>3+</sup>, Dy<sup>3+</sup>, Tb<sup>3+</sup> ions were prepared via a high temperature solid state reaction route. The compositions, photoluminescence properties, decay lifetime, thermal stability and luminous efficiency of the phosphors were investigated. For Ce<sup>3+</sup>, Dy<sup>3+</sup>/Tb<sup>3+</sup> co-doped phosphors, energy

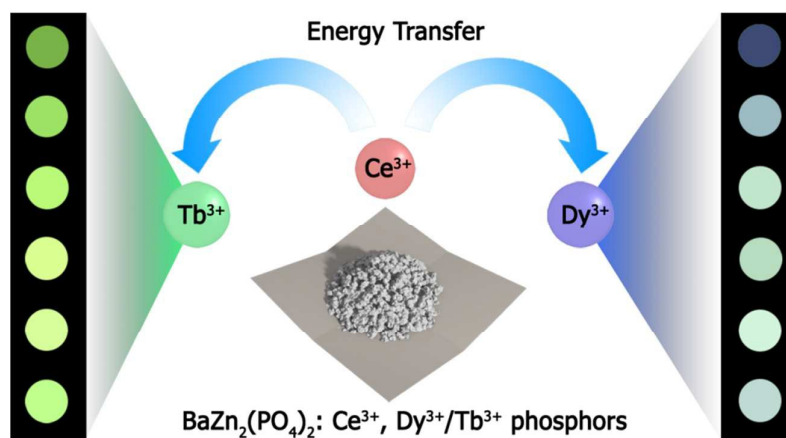
transfer from Ce<sup>3+</sup> to Dy<sup>3+</sup> and Tb<sup>3+</sup> ions was deduced by overlapping the Ce<sup>3+</sup> emission and Dy<sup>3+</sup>/Tb<sup>3+</sup> excitation spectra, which was confirmed by the decrease of Ce<sup>3+</sup> luminescence decay lifetime with increasing Dy<sup>3+</sup>/Tb<sup>3+</sup> concentration. Tunable emission from blue to bluish white and green can be realized by energy transfer and changing the doping concentrations of Dy<sup>3+</sup> and Tb<sup>3+</sup>. The energy transfer mechanism between Ce<sup>3+</sup>-Dy<sup>3+</sup>/Tb<sup>3+</sup> is demonstrated to be electric dipole-dipole interaction. The critical distances are calculated to be 21.69 Å and 19.07 Å via spectral overlap method. The result agrees well with that of 20.52 Å and 18.29 Å obtained through concentration quenching. The novel phosphors demonstrated an excellent thermal stability and outstanding luminescence properties, which points to its high potential as phosphors in the lighting field.

### Acknowledgements

This work was financially supported by the National Science Foundation of China (21266030), the Achievement Transformation Project of Xinjiang province (201154141), the Technological Innovation Youth Training Project of Xinjiang Autonomous (2013731006), and the Research Fund for the Doctoral Program of Higher Education of China (20126501120003).

### Notes and references

- H. A. Hoppe, *Angew. Chem. Int. Ed. Engl.*, 2009, **48**, 3572.
- M. M. Shang, C. X. Li, and J. Lin, *Chem. Soc. Rev.*, 2014, **43**, 1372.
- G. G. Li, D. L. G. M. M. Shang, C. Peng, Z. Y. Cheng, and J. Lin, *J. Mater. Chem.*, 2011, **21**, 13334.
- Z. Y. Hou, G. G. Li, H. Z. Lian, and J. Lin, *J. Mater. Chem.*, 2012, **22**, 5254.
- C. Feldmann, T. Jüstel, C. R. Ronda, and P. J. Schmidt, *Adv. Funct. Mater.*, 2003, **13**, 511.
- K. Li, M. M. Shang, D. L. Geng, H. Z. Lian, Y. Zhang, J. Fan, and J. Lin, *Inorg. Chem.*, 2014, **53**, 6743.
- W. Lu, N. Guo, Y. C. You, Q. Zhao, W. Z. Lv, M. M. Jiao, B. Q. Shao, and H. P. You, *Inorg. Chem.*, 2013, **52**, 3007.
- J. L. Zhang, Y. He, Z. X. Qiu, W. L. Zhang, W. L. Zhou, L. P. Yu, and S. X. Lian, *Dalton. Trans.*, 2014, **43**, 18134.
- G. R. Dillip, S. J. Dhoble, and B. Deva Prasad Raju, *Opt. Mater.*, 2013, **35**, 2261.
- J. Y. Wang, J. B. Wang, and P. Duan, *Mater. Lett.*, 2013, **107**, 96.
- Q. G. Xu, J. Y. Sun, D. P. Cui, Q. M. Di, and J. H. Zeng, *J. Lumin.*, 2015, **158**, 301.
- R. Y. Yang, and H. L. Lai, *J. Lumin.*, 2014, **145**, 49.
- Z. W. Zhang, C. L. Han, W. W. Shi, Y. Y. Kang, W. G. Zhang, and D. J. Wang, *J. Mater. Sci: Mater Electron.*, 2015, **26**, 1923.
- Z. G. Xia, and R. S. Liu, *J. Phys. Chem. C*, 2012, **116**, 15604.
- M. M. Shang, D. L. Geng, X. Kang, D. Yang, Y. Zhang, and J. Lin, *Inorg. Chem.*, 2012, **51**, 11106.
- C. Duan, Z. Zhang, S. Rösler, S. Rösler, A. Delsing, J. Zhao, and H. T. Hintzen, *Chem. Mater.*, 2011, **23**, 1851.
- X. L. Liu, Y. X. Liu, D. T. Yan, H. C. Zhu, C. G. Liu, C. S. Xu, Y. C. Liu, and X. J. Wang, *J. Mater. Chem.*, 2012, **22**, 16839.
- R. L. Kohale, and S. J. Dhoble, *J. Alloys. Compd.*, 2014, **586**, 314.
- S. Huang, and G. G. Li, *Opt. Mater.*, 2014, **36**, 1555.
- D. L. Geng, K. Li, H. Z. Lian, M. M. Shang, Y. Zhang, Z. J. Wu, and J. Lin, *Eur. J. Inorg. Chem.*, 2014, **11**, 1955.
- C. Liang, H. P. You, Y. B. Fu, X. M. Teng, K. Liu, and J. H. He, *Dalton. Trans.*, 2015, **44**, 8100.
- M. Y. Chen, Z. G. Xia, and Q. L. Liu, *J. Mater. Chem. C*, 2015, **3**, 4197.
- Z. P. Yang, P. F. Liu, L. Lv, Y. B. Zhao, Q. M. Yu, and X. S. Liang, *J. Alloys. Compd.*, 2013, **562**, 176.
- W. Lü, W. Z. Lv, Q. Zhao, M. M. Jiao, B. Q. Shao, and H. P. You, *J. Mater. Chem. C*, 2015, **3**, 2334.
- C. Y. Xu, Y. D. Li, Y. L. Huang, Y. M. Yu, and H. J. Seo, *J. Mater. Chem. C*, 2012, **22**, 5419.
- L. H. Yi, L. Y. Zhou, F. Z. Gong, Y. W. Lan, Z. F. Tong, and J. H. Sun, *Mater. Sci. Eng. B*, 2010, **172**, 132.
- P. L. Li, Z. J. Wang, Z. P. Yang, and Q. L. Guo, *J. Solid. State. Chem.*, 2014, **220**, 227.
- Z. J. Wang, P. L. Li, Z. P. Yang, and Q. L. Guo, *J. Lumin.*, 2012, **132**, 1944.
- A. Hemon, and G. Courbion, *J. Solid. State. Chem.*, 1990, **85**, 164.
- W. J. Yang, and T. M. Chen, *Appl. Phys. Lett.*, 2006, **88**, 101903-1.
- D. L. Dexter, *J. Chem. Phys.*, 1953, **21**, 836.
- G. Blasse, *Philips. Res. Rep.*, 1969, **24**, 131.
- M. M. Jiao, Y. C. Jia, W. Lü, W. Z. Lv, Q. Zhao, B. Q. Shao, and H. P. You, *J. Mater. Chem. C*, 2014, **2**, 90.
- K. Li, X. M. Liu, Y. Zhang, X. J. Li, H. Z. Lian, and J. Lin, *Inorg. Chem.*, 2015, **54**, 323.
- M. M. Jiao, W. Z. Lv, W. Lü, Q. Zhao, B. Q. Shao, and H. P. You, *Dalton. Trans.*, 2015, **44**, 4080.
- D. L. Geng, G. G. Li, M. M. Shang, D. M. Yang, Z. Y. Cheng, and J. Lin, *J. Mater. Chem.*, 2012, **22**, 14262.
- U. Caldino, E. Alvarez, A. Speghini, and M. Bettinelli, *J. Lumin.*, 2012, **132**, 2077.
- J. Zhou, and Z. G. Xia, *J. Mater. Chem. C*, 2014, **2**, 6978.



Tunable emission from blue to bluish white and green can be realized by energy transfer and changing the doping concentrations of  $\text{Dy}^{3+}$  and  $\text{Tb}^{3+}$  in  $\text{BaZn}_2(\text{PO}_4)_2$  phosphors.